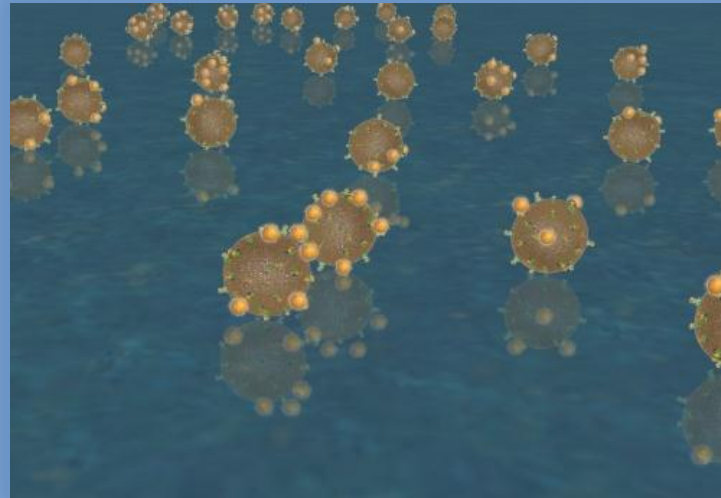


Quantifying Lipid Contents in Enveloped Virus Particles with Plasmonic Nanoparticles

Amin Feizpour

Reinhard Lab

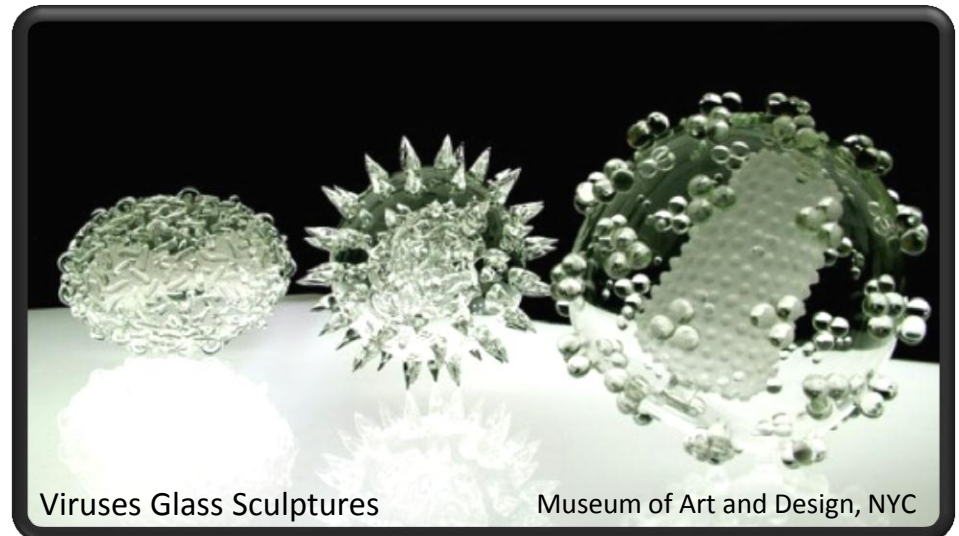
Department of Chemistry and the Photonics Center, Boston University, Boston, MA



May 2014

Outline

1. Introduction
2. Experimental & Results
3. Discussion & Summary



“... made as objects to hold, to contemplate the impact of the disease upon humanity.”

-Luke Jerram

Introduction

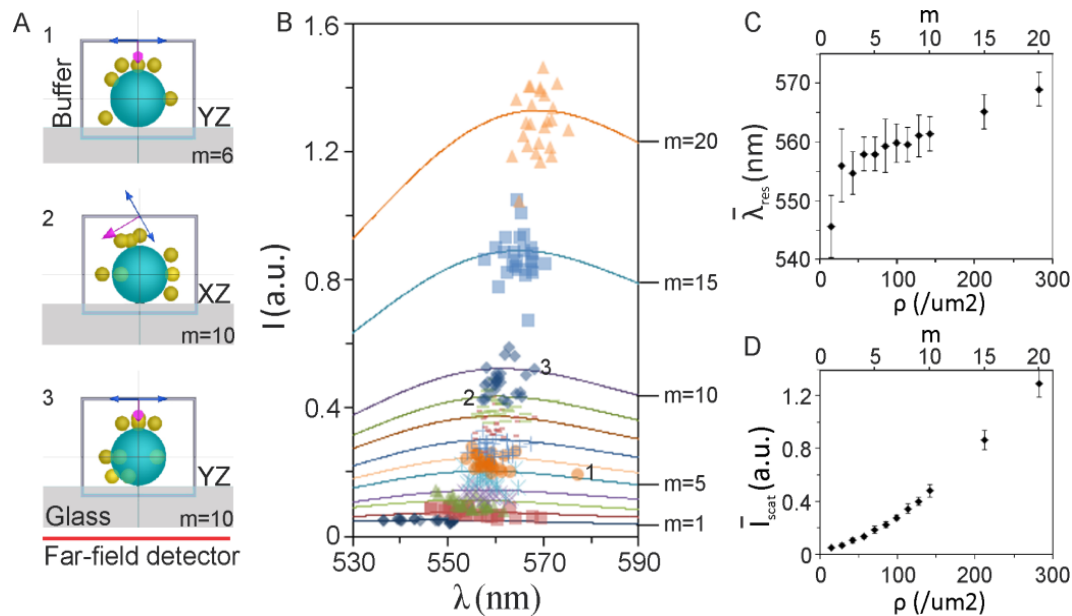
- The host-derived membrane of an enveloped virus contributes a lot to the infection mechanism.
- Phosphatidylserine (PS) has been shown to facilitate apoptotic mimicry and enhance glycoprotein-independent uptake of vaccinia, ebola and dengue viruses, and is a cofactor in infection of HIV-1.
- GSLs (GM₁, GM₃, etc.) enable the glycoprotein-independent binding of HIV-1 particles to dendritic cells.
- It is difficult to meet the concentration requirements for electrospray ionization mass spectroscopy (ESI-MS), the analytical method of choice in lipidomics using human-isolated virus samples.

- Mercer J & Helenius A (2010) Apoptotic mimicry: phosphatidylserine-mediated macropinocytosis of vaccinia virus. *Ann. N.Y. Acad. Sci* 1209:49-55.
- Moller-Tank S, Kondratowicz AS, Davey RA, Rennert PD, & Maury W (2013) Role of the Phosphatidylserine Receptor TIM-1 in Enveloped-Virus Entry. *Journal of Virology* 87:8327-8341.
- Jemielity S, *et al.* (2013) TIM-family proteins promote infection of multiple enveloped viruses through virion-associated phosphatidylserine. *PLoS Pathog* 9(3):e1003232.
- Callahan MK, *et al.* (2003) Phosphatidylserine on HIV envelope is a cofactor for infection of monocytic cells. *J Immunol* 170(9):4840-4845.
- Puryear WB, *et al.* (2012) Interferon-Inducible Mechanism of Dendritic Cell-Mediated HIV-1 Dissemination is Dependent on the Siglec, CD169. *PLoS Pathogens* accepted, PPATHOGENS-D-12-03047R1.
- Puryear WB, Yu X, Ramirez NP, Reinhard BM, & Gummuluru S (2012) HIV-1 incorporation of host-cell-derived glycosphingolipid GM3 allows for capture by mature dendritic cells. *Proceedings of the National Academy of Sciences of the U.S.A* 109:7475-7480.
- Brugger B (2014) Lipidomics: Analysis of the Lipid Composition of Cells and Subcellular Organelles by Electrospray Ionization Mass Spectrometry. *Annual review of biochemistry*.

Experimental & Results

1. Simulation Results
2. VLPs panel studied in this research
3. Sample prep and EM imaging
4. Optical Setup and Spectral measurement and analysis
5. Calibration on liposomes
6. Measurement of lipid contents on 4 different VLPs

Simulation Results



The simulation of the far-field scattering response of GNPs on a VLP.

(A) 3 of the random distributions of GNPs on the surface of a VLP,

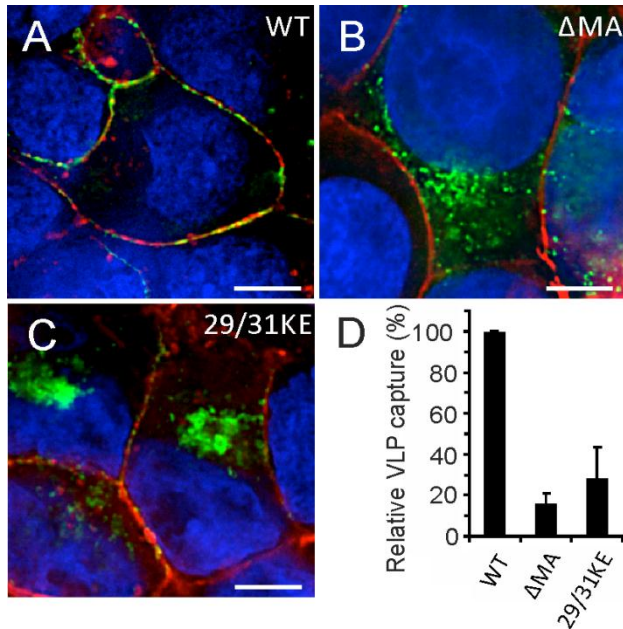
(B) The distribution of the peak wavelengths and intensities (markers) of all the GNP/VLP complexes studied containing 1 to 20 GNPs per VLP, each with 25 different configurations. The curves show the spectra each as an average of the 25 spectra obtained for a single m and 25 different configurations. The numbers show the data points corresponding to the 3 example complexes.

(C) The average peak wavelength as a function of density of GNPs per VLP.

(D) The average peak intensity as a function of density of GNPs per VLP. Error bars show the standard deviation of the peak value, in 25 simulations per m , from average.

VLPs panel studied in this research

1. Wild Type (**WT**) Gag-eGFP HIV-1 VLPs
2. **PDMP** VLPs generated in threo-1-phenyl-2-decanoylamino-3-morpholino-1-propanol (PDMP) treated host cells
3. **29/31KE** VLPs (two lysine to glutamate changes in MA head)
4. **Δ MA** VLPs (15-99 basic amino acids in MA head deleted)

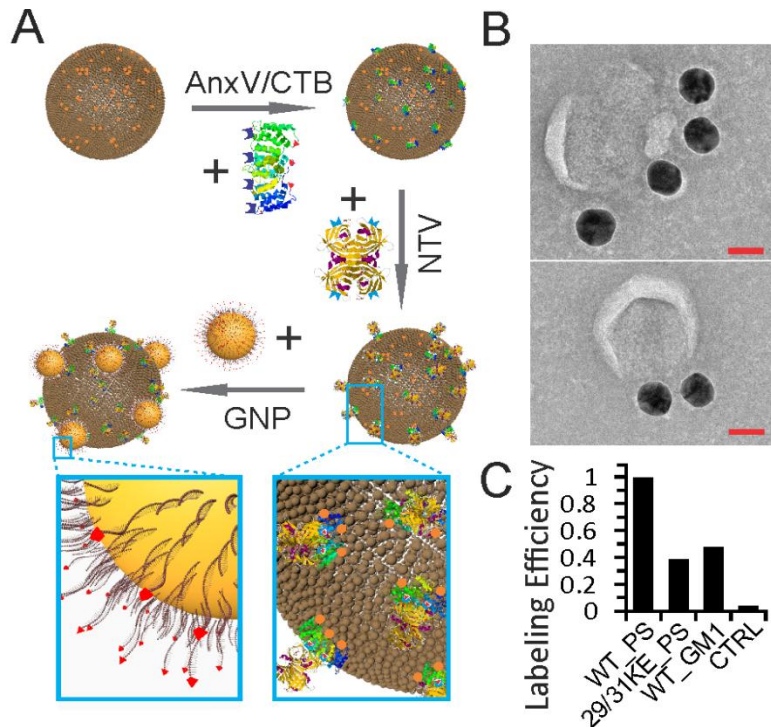


Mutations in the matrix domain of the Gag redirect the formation of VLPs from plasma membrane to intracellular compartments.

Fluorescence images of HEK293T cells 1 day post transfection with (A) WT, (B) Δ MA and (C) 29/31KE VLPs. Virus, membrane and nucleus were stained in green, red and blue, respectively. In (A) WT Gag colocalizes with the plasma membrane where WT VLPs assemble. In contrast, Δ MA and 29/31KE VLPs in (B) and (C) are associated with intracellular compartments.

(D) Relative capture of WT, Δ MA and 29/31KE VLPs by DCs.

Sample prep and EM imaging and quantification



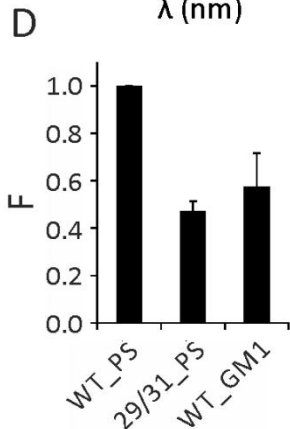
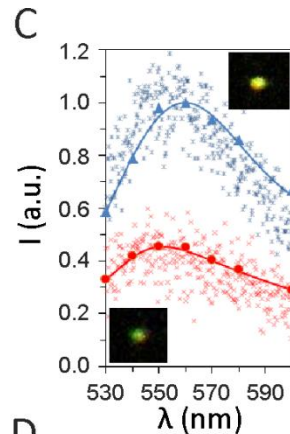
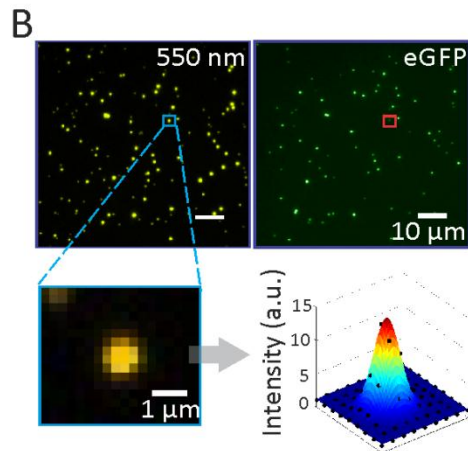
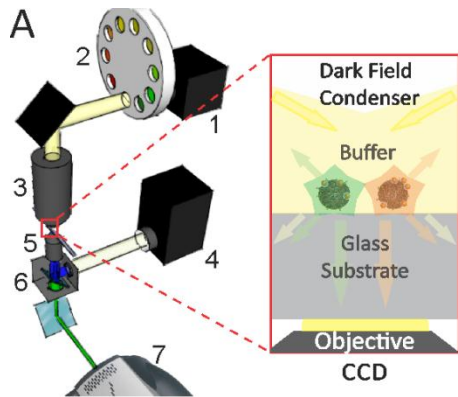
The experiment design and validation of GNP/VLP binding through electron microscopy.

(A) The VLPs after being functionalized by either Annexin V or Cholera Toxin B and neutravidin were randomly attached on glass substrate and incubated with Biotin-ssDNA-GNPs colloid for 15 min.

(B) HRTEM imaging on a fixed negatively-stained sample showed the presence of multiple GNPs per VLP where the PS lipid was targeted on WT VLPs. Scale bars are 40 nm.

(C) The numbers of GNPs per VLP for 3 different samples and a negative control were quantified through SEM imaging. These samples included targeting PS lipid on WT and 29/31KE VLPs and G_{M1} lipid on WT VLPs.

Optical Setup and Spectral measurement and analysis



The optical setup used to measure the far-field scattering spectra together with fluorescence localization.

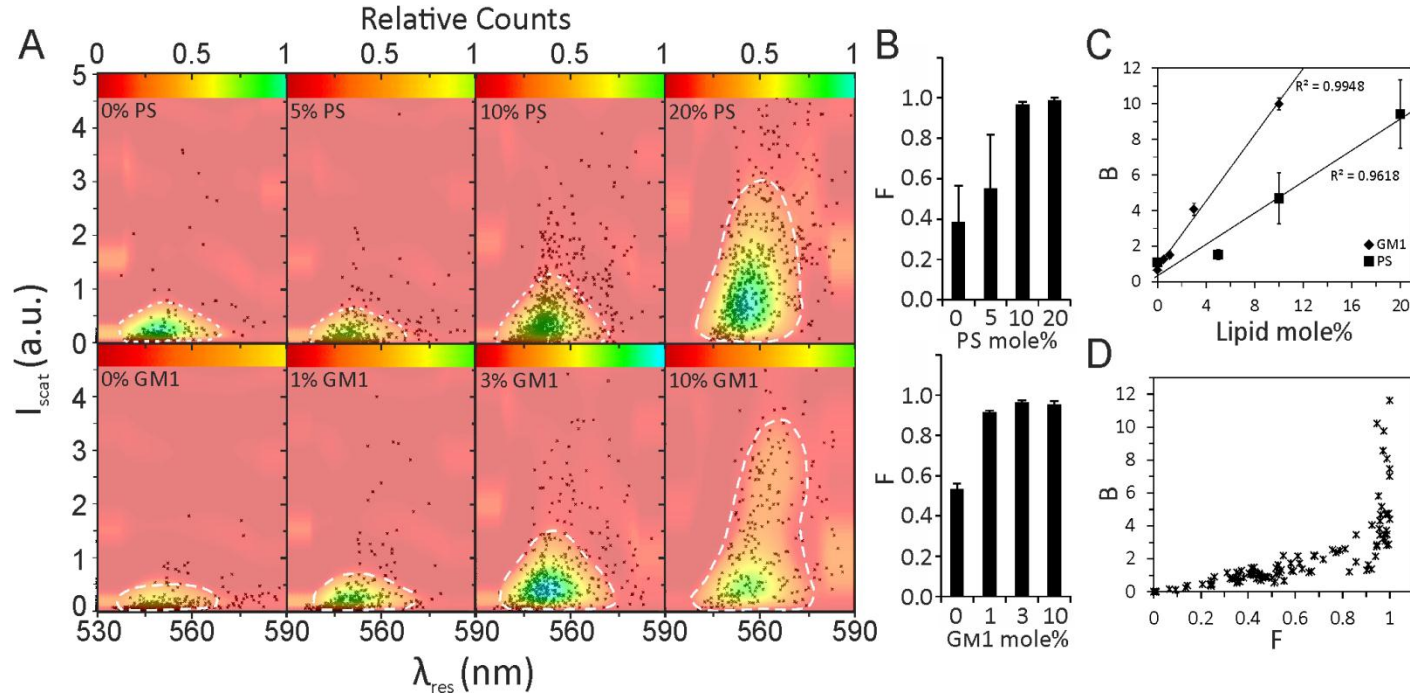
(A) The microscope setup including a filter wheel on top for multi-spectral imaging and fluorescence imaging apparatus in the bottom. Inset: the schematic representation of two VLPs with different densities of GNPs on the surface and hence different scattering colors. Labels: 1-Tungsten lamp, 2-Filter wheel, 3-Light condenser, 4-Mercury lamp, 5-60x oil objective, 6-Fluorescence filter set, 7-EMCCD.

(B) One of the 9 scattering images obtained in the 530 to 600 nm range from a sample of WT VLPs with GNPs targeting their PS lipids and its corresponding fluorescence image showing the locations of the VLPs. Inset: the scattering cross section of one of the VLPs and its corresponding point spread function (PSF) obtained by Gaussian surface fitting for intensity measurement.

(C) Two of the spectra obtained through multi-spectral imaging and curve fitting (large markers and lines), and conventional optical spectrometry (small markers), for two VLPs with different densities/configurations of GNPs on the surface show nicely correlated results.

(D) The binding probability, F , obtained through 3 or more optical measurements ($n \geq 3$) of 3 different samples.

Calibration on liposomes



Calibration of the optical measurement of binding using liposomes.

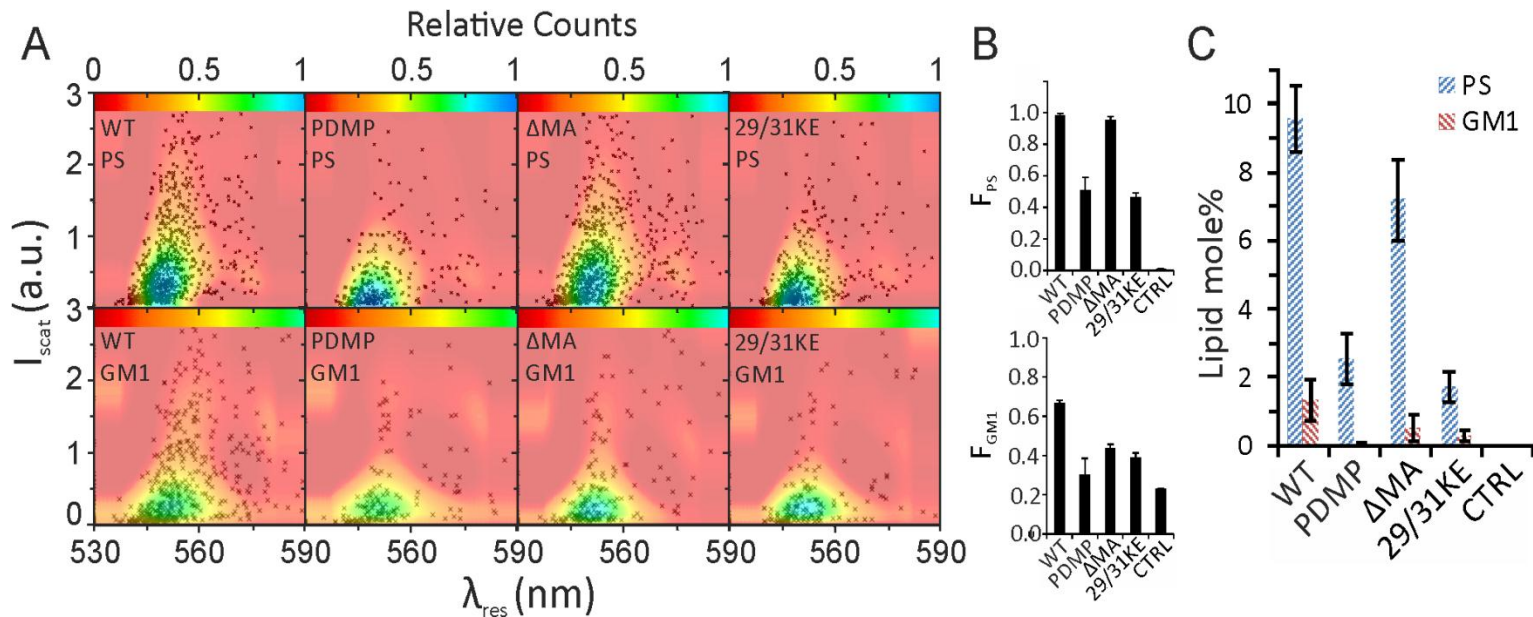
(A) The distribution of peaks of the spectra measured for liposomes with varying PS concentrations from 0 to 20% and varying G_{M1} concentration from 0 to 10% and labeled with GNPs, in black markers, and a surface fitting on their distribution in the color map. The white dashed lines show the area of each plot that contains by average 90% of the data points, $A_{90\%}$, used as a metric for the amount of plasmon coupling. Each plot shows the data of all different runs of the same measurement which contain 500-1500 liposomes in total.

(B) The fraction of labeled liposomes or binding probability, F , in different samples.

(C) The calibration curves obtained based on calculation of the B value for each liposome binding sample, that show linear trends in the measured range.

(D) The binding value, B , as a function of the binding probability, F , as obtained from tens of different experiments on various samples of VLPs and liposomes in this study. Each sample was measured in 3 independent runs ($n=3$).

Measurement of lipid contents on 4 different HIV-1 VLPs



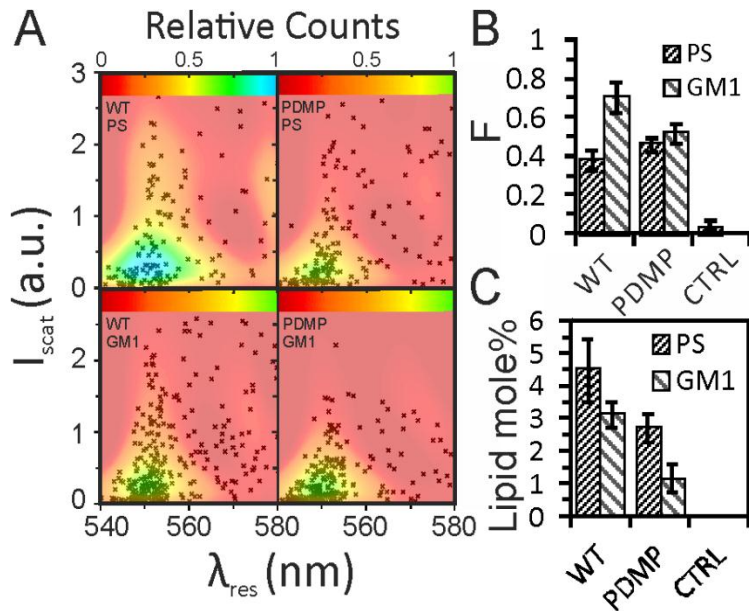
Optical measurement of the PS and G_{M1} contents in 4 different HIV-1 VLPs.

(A) The scatter plots of the peaks, in black markers, and their distribution surfaces in color maps for PS and G_{M1} quantification in the 4 VLPs. Each plot contains the data of 500-1500 VLPs obtained in 3 or more runs of the experiment ($n \geq 3$).

(B) The F values associated with the same measurements.

(C) The results of PS and G_{M1} quantification after calibration of the B values of the 8 samples, using the calibration functions obtained through liposomes.

Lipid quantification on two Ebola VLPs



Optical measurement of the PS and G_{M1} contents in 2 different Ebola VLPs.

(A) The scatter plots of the peaks, in black markers, and their distribution surfaces in color maps for PS and G_{M1} quantification in the 2 VLPs. Each plot contains the data of 500-700 VLPs obtained in 3 runs of the experiment ($n=3$).

(B) The F values associated with the same measurements.

(C) The results of PS and G_{M1} quantification after calibration of the B values of the samples.

Discussion & Summary

- Our method, based on spectral analysis of gold nano-label binding and plasmon coupling, allows for measuring the lipid contents of viral envelopes through a rather simple and rapid protocol which leads to precise results.
- The simulations of the far-field scattering spectra showed ~25 nm spectral red-shift and 26-fold intensity boost by increasing the number of bound GNPs from 1 to 20.
- This, experimentally, provided a broad dynamic range of lipid concentration measurements from approximately 1 to 20 mole% in this study.
- We have used less than 10^7 VLPs per experiment in this study, equal to the amount of virus particles that can be normally obtained from less than 10 mL of patient blood.
- The detection limit of this assay with the settings of this study is approximately 1% lipid.
- The PS concentrations detected on the VLPs were in agreement with other researches and correlated with the budding sites of the viruses.
- The GM₁ was quantified for the first time and it's correlated with the amount of capture of the VLPs by mDCs.
- The method can be generalized to other viruses with slight modifications.